SAE International

2012-01-1152
Published 04/16/2012

doi:10.4271/2012-01-1152
saefuel.saejournals.org

Dual-Injection as a Knock Mitigation Strategy Using Pure Ethanol and Methanol

Ritchie Daniel, Chongming Wang and Hongming Xu
University of Birmingham

Guohong Tian
Newcastle University

Dave Richardson
Jaguar Cars Ltd

ABSTRACT

For spark ignition (SI) engines, the optimum spark timing is crucial for maximum efficiency. However, as the spark timing is advanced, so the propensity to knock increases, thus compromising efficiency. One method to suppress knock is to use high octane fuel additives. However, the blend ratio of these additives cannot be varied on demand. Therefore, with the advent of aggressive downsizing, new knock mitigation techniques are required. Fortuitously, there are two well-known lower alcohols which exhibit attractive knock mitigation properties: ethanol and methanol. Both not only have high octane ratings, but also result in greater charge-cooling than with gasoline. In the current work, the authors have exploited these attractive properties with the dual-injection, or the dual-fuel concept (gasoline in PFI and fuel additive in DI) using pure ethanol and methanol. The single cylinder engine results at 1500 rpm (λ=1) show benefits to indicated efficiency and emissions (HC, CO and CO_2) at almost every load (4.5 bar to 8.5 bar IMEP) compared to GDI. This is because the spark timing can be significantly advanced despite the use of relatively low blends ($\leq$50%, by volume), which lowers the combustion duration and improves the conversion of fuel energy into useful work. Overall, these results reinforce the potential of the dual-injection concept to provide a platform for aggressive downsizing, whilst contributing to a renewable energy economy.

CITATION: Daniel, R., Wang, C., Xu, H., Tian, G. et al., "Dual-Injection as a Knock Mitigation Strategy Using Pure Ethanol and Methanol," *SAE Int. J. Fuels Lubr.* 5(2):2012, doi:10.4271/2012-01-1152.

INTRODUCTION

In order to increase regional energy security and combat rising global CO_2 emissions, there is an increasing need to revolutionize the energy supply chain. This adds to the underlying concern that, based on current trends, leading energy forecasters expect the world's petroleum to be depleted within the next 40 years [1, 2]. Therefore, it is paramount to search for alternative energy sources in order to alleviate environmental stress and confront the ballooning energy demand. In the UK, it is believed that biofuels offer the most viable mid-term supplement or substitute for gasoline, compared to technologies which are in their infancy (hydrogen fuel cells and full electric platforms) [3].

Although the idea of fuelling internal combustion engines with biofuels is not new [4], its use is receiving increased worldwide attention. Liquid biomass offers a high energy density option and is compatible with existing combustion systems. In Europe, the promotion of biofuels has led to a legislative approach; by 2020, all EU member states must conform to a 10% minimum target on the use of alternative fuels (biofuels or other renewable fuels) in transportation [5]. In the US, tax incentives have been used to promote the use of ethanol in gasoline [6], in an effort to replicate the success seen in Brazil [7]. Therefore, more emphasis is being placed on the automotive sector to not only design compatible systems with these alternative fuels, but to also optimize their use in neat form and in blends with gasoline.

Currently, ethanol is the most widely adopted biofuel [8, 9]. In 2007, ethanol accounted for 80% of the world's total biofuel production [10]. In Brazil, where its use has dramatically reduced the dependency on petroleum, ethanol is

used as a neat engine fuel or in various blends with gasoline [11, 12]. Alternatively, China has focused on the use of methanol and leads the world as a producer and consumer [13]. This is largely due to the lack of grain and abundance of coal, as opposed to favoring the performance of methanol over ethanol. Nevertheless, low methanol blends with gasoline (up to 15%) have been shown to require only minor engine modifications [14] and yield similar fuel performance to gasoline [15, 16].

In order to maximize the use of these alternative fuel options to gasoline, the automotive industry is beginning to focus on their optimal combustion in spark ignition (SI) engines. An area of keen interest is the method of fuel supply to the engine. Traditionally, in terms of fuel injection, the approach has mirrored that with gasoline; the alternative fuel, in neat or blended form, is injected using either port fuel injection (PFI) or direct-injection (DI). Alternatively, flexible fuelled ethanol vehicles, used ubiquitously in Brazil, can permit a variable blend of ethanol and gasoline (mixed in the fuel tank), as the actual blend can be detected by the diagnostics system [17]. However, the blend ratio cannot be varied in real-time using the engine control unit (ECU), as it is only measured. Therefore, alternative fuelling approaches are being investigated, including that of dual-injection; the combined use of PFI and DI to supply online gasoline-biofuel blends. By leveraging both injection systems simultaneously, instantaneous blend ratios can be supplied to the engine to best suit the duty cycle. In principle, dual-injection combines the advantages of both bi-fuel and flex-fuel approaches.

The potential of dual-injection inspired the creation of Ethanol Boosting Systems (EBS) LLC in 2006. Here, the researchers, who mainly originate from Massachusetts Institute of Technology (MIT), have examined the potential of ethanol (hydrous and anhydrous) boosted direct- and dual-injection engines, to help cool the charge and suppress knock, with only modest hardware modifications [18, 19, 20]. Ford is also investigating the dual-injection technology on their 'Ecoboost' gasoline turbo-charged direct-injection (GTDI) engines. Here, PFI gasoline and DI E85 (15% gasoline and 85% ethanol, by volume) has been used to improve the engine efficiency and to avoid knock at high load [21, 22]. Other original equipment manufacturers (OEMs) that have investigated the combination of PFI and DI fuelling include Toyota and more recently, Audi. The work by Toyota demonstrated the improved engine performance (fuel economy and torque) and reduced emissions at full load using a 3.5 liter V6 gasoline engine (2GR-FSE) [23]. For Audi, the dual-injection technique is being used in a turbocharged 1.8 liter gasoline engine. As with the 2GR-FSE engine, this combustion mode contributes to higher fuel efficiencies at part-load compared to conventional single injection [24]. Clearly, the benefits of dual-injection arise when the engine duty cycle includes frequent medium- to high-load operation.

Most investigations of dual-injection have included ethanol as the DI fuel for knock mitigation purposes. However, the use of methanol can also greatly increase the charge-cooling effect and therefore knock suppression in order to support PFI gasoline. With recent industry focus on engine downsizing, it is more important to mitigate knock. The team from EBS LLC have conducted modeling studies of alcohol fuels in a highly turbo-charged DISI engines which could be used in heavy duty long haul applications [25]. They have suggested that turbo-charged DI alcohol engines could be as, or more efficient, than diesel engines. The team have also produced simulation results comparing E85 and methanol in collaboration with Volvo [26]. Their simulation results showed how methanol might be more effective than E85 (for the same knock suppression, only half the fuel flow of methanol is required). However, these numerical calculations have not been compared with experimental work.

Therefore, it is the aim of this paper to experimentally compare the dual-injection strategy when using ethanol and methanol as knock mitigation fuels in dual-injection using a single cylinder SI research engine. The effectiveness of each alcohol is assessed as a knock mitigation fuel for PFI gasoline. The approach is to use minimum alcohol injections so that the knock limit is raised from PFI gasoline. The engine performance and emissions are compared at various engine loads from 3.5 bar to 8.5 bar IMEP in 1 bar intervals. In the following sections, the engine setup, experimental results and finally conclusions are discussed.

EXPERIMENTAL SETUP

ENGINE AND INSTRUMENTATION

The experiments were performed on a single-cylinder, 4-stroke SI research engine, as shown in Figure 1.

The 4-valve cylinder head includes the Jaguar spray-guided direct-injection (SGDI) technology used in their V8 production engine (AJ133) [27]. It also includes variable valve timing technology for both intake and exhaust valves, which, for this study, was kept constant, as shown in Table 1. As well as firing under high pressure (150 bar) SGDI conditions, a low pressure (3 bar) PFI system is available. The two fuelling modes can be used independently or simultaneously, as in the case for dual-injection.

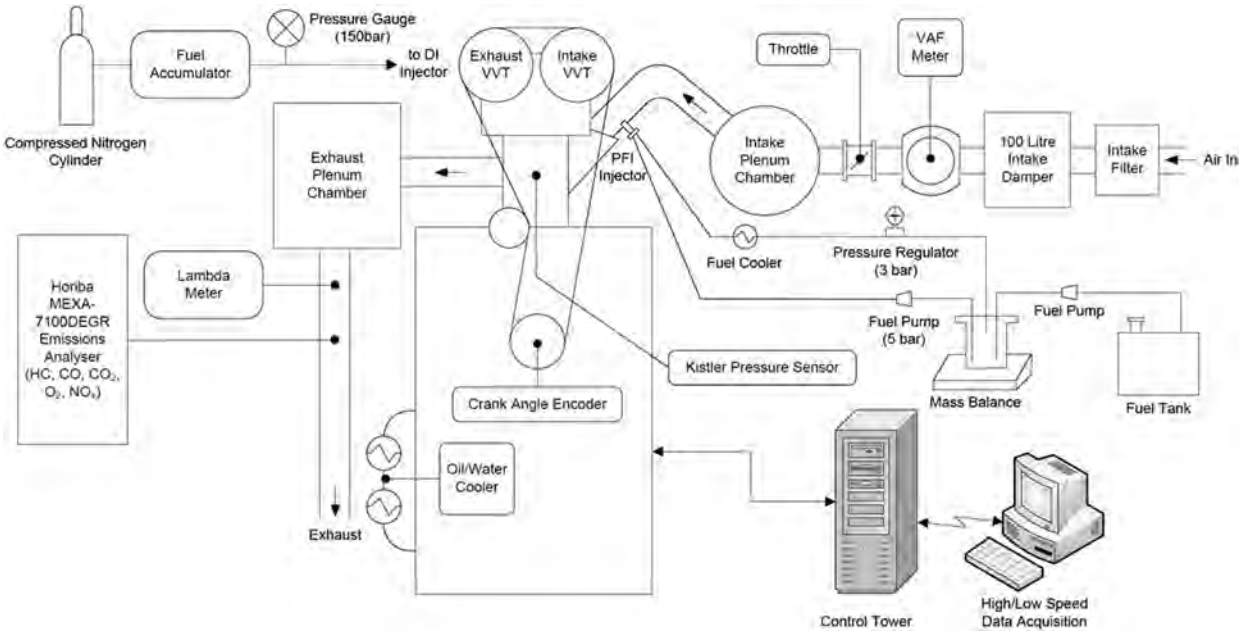

Figure 1. Schematic of engine and instrumentation setup

Table 1. Engine Specification

Engine Type	4-Stroke, 4-Valve
Combustion System	Dual-Injection: PFI and Spray-Guided DISI
Swept Volume	565.6 cm^3
Bore x Stroke	90 x 88.9 mm
Compression Ratio	11.5:1
Engine Speed	1500 rpm
Injector	Multi-Hole Nozzle
PFI Pressure and SOI Timing	3 bar, 50º $bTDC_{comb}$
DI Pressure and SOI Timing	150 bar, 280º $bTDC_{comb}$
Intake Valve Opening	16º $bTDC_{intake}$
Exhaust Valve Closing	36º $aTDC_{intake}$
Valve Open Duration	250 CAD

The engine was coupled to a DC dynamometer to maintain a constant speed of 1500 rpm (±1 rpm) regardless of the engine torque output. The in-cylinder pressure was measured using a Kistler 6041A water-cooled pressure transducer which was fitted to the side-wall of the cylinder head. The signal was then passed to a Kistler 5011 charge amplifier and finally to a National Instruments data acquisition card. Samples were taken at 0.5 crank angle degree (CAD) intervals for 300 consecutive cycles, so that an average could be taken. The crankshaft position was measured using a digital shaft encoder mounted on the crankshaft. Coolant and oil temperatures were controlled at 85 ±5°C and 95 ±3°C, respectively, using a Proportional Integral Differential (PID) controller. All temperatures were measured with K-type thermocouples.

The engine was controlled using software developed in-house written in the LabVIEW programming environment. High-speed, crank-angle-resolved and low-speed, time-resolved data was also acquired using LabVIEW. This was then analyzed using MATLAB developed code so that an analysis of the combustion performance could be made.

EMISSIONS AND FUEL MEASUREMENT

The gaseous emissions were quantified using a Horiba MEXA-7100DEGR gas analyzer. Exhaust samples were taken 0.3m downstream of the exhaust valve and were pumped via a heated line (maintained at 191°C) to the analyzer.

The fuel consumption rate and resulting blend ratios were calculated using the volumetric air flow rate (measured by a positive displacement rotary flow meter and stabilized by a 100 L intake plenum), known DI injector calibration curves for each fuel and the lambda (λ) value. All tests were run at stoichiometric conditions (λ=1), which was controlled using the cross-over of the carbon monoxide (CO) and oxygen (O_2) emissions concentrations, as described in detail in a previous publication by the authors [28].

TEST FUELS

Both 97 RON gasoline and ethanol were supplied by Shell Global Solutions, UK, whereas the methanol was supplied by Fisher Scientific, UK (99.5% purity). A high octane gasoline was chosen as this represents the most favorable characteristics offered by the market and provides a competitive benchmark to the lower alcohols. The fuel characteristics are shown in Table 2.

Table 2. Test Fuel Properties

	Ethanol	Methanol	Gasoline
Chemical Formula	C_2H_6O	CH_4O	$C_{6.62}H_{11.88}$
H/C Ratio	3	4	1.795
O/C Ratio	0.5	1	0
Gravimetric Oxygen Content (%)	34.78	50	0
Density @ 20ºC (kg/m^3)	790.9*	792	744.6
Research Octane Number (RON)	107†	106†	96.8
Motor Octane Number (MON)	89†	92†	85.7
Anti-Knock Index	98	99	91.25
Stoichiometric Air Fuel Ratio	8.95	6.47	14.46
LCV (MJ/kg)	26.9*	19.83*	42.9
LCV (MJ/L)	21.3*	15.7*	31.9
Carbon Intensity (gCO_2/MJ)	71	69.4	74.4
Flash Point (ºC)	13	12	-40
Heat of Vaporization (kJ/kg)	840†	1103†	373
Stoichiometric Heat of Vaporization (kJ/kg_{air})	93.9	171.5	25.8
Initial Boiling Point (ºC)	78.4	65	32.8

**Measured at the University of Birmingham: ASTM D240*
†Heywood, J.B., Internal Combustion Engine Fundamentals. 1988: McGraw-Hill [29]

FUELLING VARIATIONS

For clarity, the fuelling variations used in this work (3 fuels and 3 injection modes) have been abbreviated in the remaining sections. When gasoline has been used in PFI and DI it is referred to as PFI and GDI, respectively. When referring to either lower alcohol used as a neat DI fuel, the notation EDI and MDI is used for ethanol and methanol, respectively. To indicate ethanol and methanol dual-injection, the first letter of each is positioned after the first letter in GDI (which indicates gasoline) and is separated with a hyphen. For instance, ethanol dual-injection (PFI + EDI) is denoted G-EDI. A summary of this information is found in Table 3.

Table 3. Fuelling Variations

PFI Fuel	DI Fuel	MBT Timing	Notation
Gasoline		PFI	PFI
	Gasoline	GDI	GDI
	Ethanol	EDI	EDI
	Methanol	MDI	MDI
Dual-Injection			
Gasoline	Ethanol	EDI	G-EDI
Gasoline	Methanol	MDI	G-MDI

EXPERIMENTAL PROCEDURE

The engine was considered warm once the coolant and lubricating temperatures had stabilized at 85°C and 95°C, respectively. All the tests were carried out at the stoichiometric air-fuel ratio (AFR_{stoich}), or λ=1, fixed injection timing (280°bTDC_{comb}) and engine speed (1500 rpm), ambient air intake conditions (approximately 25 ±2°C) and constant valve timing (see Table 1). The ignition timings for G-EDI and G-MDI were equal to the MBT timings of EDI and MDI, respectively (see Table 3). This represents the maximum improvement in efficiency (from PFI) with the minimum amount of alcohol injection. Therefore, the authors intend to examine the volume fraction of alcohol required to reach the same level of knock mitigation as EDI and MDI. As a consequence of this effective knock suppression, this method helps to minimize the increase in fuel consumption over PFI gasoline (the lower alcohols have lower LCVs, see Table 2). The in-cylinder pressure data from 300 consecutive cycles was then averaged and analyzed using the aforementioned MATLAB script.

When changing fuels, the high pressure DI fuelling system was purged using nitrogen until the lines were considered clean. As a further precaution, the new DI fuel was then flushed through the high pressure circuit in order to dilute the effect of any previous fuel. Once the line was re-pressurized to 150 bar using the new DI fuel, the engine was run for several minutes. This made sure that no previous fuel remained on the injector tip or any combustion chamber crevices before any data was acquired. Each test was also run three times for repeatability.

FUEL BLEND CALCULATIONS

In research, the air-fuel ratio (AFR) of a known fuel composition is conventionally measured using an appropriate lambda meter and oxygen sensor. This requires presetting the AFR_{stoich} value for either neat fuel or the known fuel blend. However, in this study, the exact in-cylinder blend ratio of the two fuels from PFI and DI varies as required and the overall composition is therefore unknown prior to testing. Therefore, the authors have used the cross-over theory of the O_2 and CO emissions concentrations, instead of the lambda meter and oxygen sensor combination, to control the excess air ratio under steady-state conditions. For transient engine

testing, a fast response O_2 and CO emissions analyzer is necessary.

This cross-over theory is not new, and is described in comprehensive engine textbooks [29, 30]. It is based on the theory that close to stoichiometry, the O_2 and CO emissions concentrations are equal. When the mixture is lean, excessive air helps to oxidize the CO. Conversely, as the mixture becomes rich in fuel, the O_2 content decreases and the CO production increases inversely. Therefore, in the event of an AFR sweep, the O_2 and CO emissions concentrations can be shown by two separate curves which cross-over close to stoichiometry. Previous work by the authors confirms that this cross-over theory can be used to control the in-cylinder blend ratio of oxygen content fuels (such as ethanol and methanol) with gasoline [28].

As previously mentioned, the blend ratio in this work was measured after the testing. Therefore, in order to calculate this blend ratio, the fuel flow rates for the PFI and DI components were needed. To achieve these flow rates, the authors have made two assumptions. Firstly, the blending AFR_{stoich} and LCVs were assumed linear between each fuel. Secondly, the DI injector mass flow rates were estimated for each blend using the calibration curves for each fuel, if an offset is applied to the 100% DI case. This is because the injector tip is affected by local conditions during the experiments. Therefore, this offset adjusts the calibrated flow rates for improved accuracy in the absence of a flow meter. The high pressure DI injector used in the experiments was individually calibrated using ethanol and methanol from 0.3-6ms. Although the results were near linear down to very low pulse widths (0.3ms), the only operating points to require pulse widths below 0.5ms was at 4.5bar IMEP.

Now that the DI fuel flow rate can be accurately obtained, along with the air flow rate and relative AFR (λ), the gasoline fuel mass in PFI can be inferred using Equation 1:

$$\lambda = \frac{AFR_{actual}}{AFR_{stoichiometric}} = 1 \qquad (1)$$

Therefore, for a given fuel blend with gasoline in PFI and the lower alcohol (ethanol or methanol) in DI, this equation becomes:

$$\lambda = \frac{\left(\frac{m_a}{m_{f,DI}+m_{f,PFI}}\right)}{\left[\left(\frac{m_{f,DI}}{m_{f,DI}+m_{f,PFI}}\right)AFR_{s,DI}+\left(\frac{m_{f,PFI}}{m_{f,DI}+m_{f,PFI}}\right)AFR_{s,PFI}\right]}$$

$$\therefore \quad \lambda = \frac{m_a}{(m_{f,DI})AFR_{s,DI}+(m_{f,PFI})AFR_{s,PFI}} \qquad (2)$$

In Equation 2, m_a and m_f denote the mass of air and fuel (in PFI and DI), respectively. Equation 2 can then be simplified and re-arranged to find the mass of gasoline in PFI ($m_{f,PFI}$), as shown in Equation 3:

$$m_{f,PFI} = \frac{m_a-(m_{f,DI})AFR_{s,DI}}{AFR_{s,PFI}} \qquad (3)$$

It is now possible to calculate the fuel blend, as both PFI and DI components are known.

RESULTS AND DISCUSSION

ETHANOL VS. METHANOL DUAL-INJECTION

Single component fuels with a high latent heat of vaporization, like ethanol and methanol, can help to suppress the knock encountered with PFI when used in dual-injection mode. However, without knowing the exact blend composition, the authors have relied on the cross-over of the CO and O_2 concentrations to control stoichiometry. From previous investigations, the authors found that stoichiometry can be controlled to within 1% error (lambda, λ = 1 ±0.01) when the difference between the CO and O_2 concentrations was within ±0.1% [28]. For this work, the CO and O_2 concentration cross-over for each G-EDI and G-MDI test point is within this error, as disclosed in Figure 2.

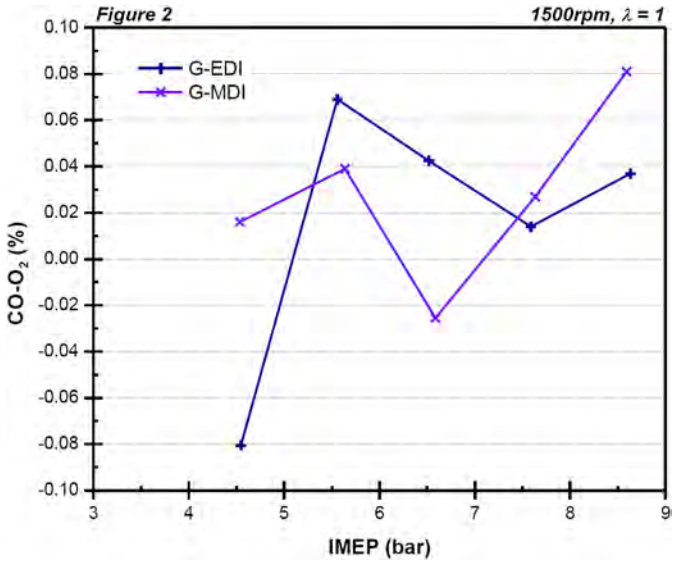

Figure 2. Differences between carbon monoxide and oxygen emissions concentrations for G-EDI and G-MDI

Having accurately located stoichiometry for G-EDI and G-MDI, the minimum DI volume fractions are then calculated (in order to reach the same MBT timings as EDI and MDI, respectively). These results are shown in Figure 3a. Clearly, the DI volume fractions increase with increasing load because the need to suppress knock is greater as the spark advance required from PFI increases. Both lower

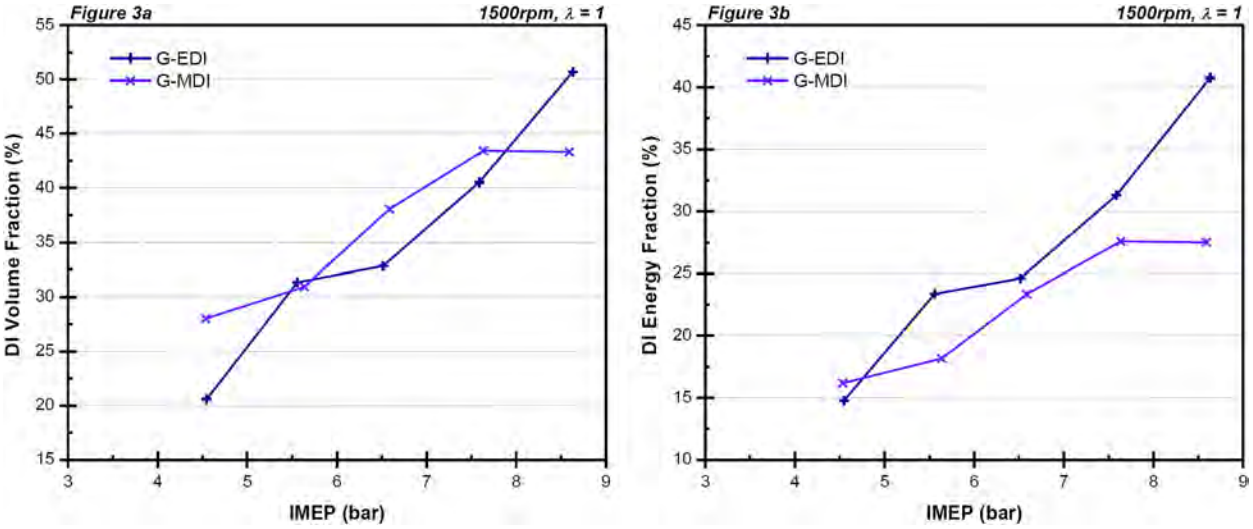

Figure 3. Volume (a) and energy (b) fractions of DI components in G-EDI and G-MDI

alcohols are effective at suppressing knock. For instance, at 7.5 bar IMEP, the minimum DI volume fractions with G-EDI and G-MDI are only 41% and 43%, respectively, whilst the spark advance required to reach the MBT timing of EDI and MDI at this load is 11 CAD and 12 CAD from PFI, respectively (see Figure 4a). The reason why G-MDI requires greater DI volume fractions than with G-EDI at 6.5 bar and 7.5 bar IMEP, despite having a greater charge-cooling effect (see Table 2), is because the MBT spark timing is 1 CAD earlier. However, in terms of lower calorific value (LCV), the DI volume fractions for G-EDI and G-MDI correspond to 32% and 27% of the overall alcohol-gasoline blend LCV, respectively, as shown in Figure 3b. At the highest load (8.5 bar IMEP) this difference increases further; the energy fraction of G-EDI increases to 41%, whereas it remains at 27% with G-MDI. On this basis, a lower energy fraction is required by methanol in G-MDI than by ethanol in G-EDI, which is likely a consequence of the greater heat of vaporization of methanol compared to ethanol (see Table 2). At 4.5 bar IMEP, the DI volume fraction with G-MDI is also higher than with G-EDI. This is because methanol has a lower LCV and so more fuel is required for the same energy input (see Table 2). Nevertheless, the overall trend with G-EDI and G-MDI is very similar and the DI volume fraction is comparable with increasing engine load.

In addition to the control of stoichiometry, the minimum amount of lower alcohol in dual-injection was added until the spark timing was advanced to reach the MBT timing of its neat form in DI (EDI and MDI) was found. This knock suppression is possible because of the improved chemical reactions (higher RON and MON) and higher heat of vaporizations of the lower alcohols, as shown in Table 2. These spark timings are shown in Figure 4a. At low load (3.5 bar IMEP) gasoline in PFI is not limited by knock. Therefore, G-EDI and G-MDI is not required. Within the remaining load window (4.5 bar to 8.5 bar IMEP), the combustion of G-EDI and G-MDI is similarly not limited by knock. This therefore allows the optimum spark timing to be found, which is much more advanced than PFI. This helps to advance the combustion phasing towards the optimum location, whereby the 50% mass fraction burned (MFB) point, or CA50 is between 8-10°aTDC [31], as shown in Figure 4b.

IN-CYLINDER BEHAVIOR

In general, when advancing the spark timing, the maximum in-cylinder pressure (P_{max}) increases. For G-EDI and G-MDI, the P_{max} is shown in Figure 5. For each load, the P_{max} is much higher than PFI and GDI. This is largely due to the more advanced spark timing because of the greater charge-cooling when using ethanol and methanol as DI anti-knock supplements. At 8.5 bar IMEP, P_{max} increases to 52 bar with both lower alcohols, which is 16 bar higher than GDI. As the spark is advanced from PFI, the combustion process initiates closer to TDC. Therefore, more of the combustion process occurs at a lower in-cylinder volume, thus generating higher combustion pressures. This improves the combustion rate and increases the expansion of the combustion products into useful energy. Furthermore, throughout the entire load range, the P_{max} with G-MDI is marginally higher than that for G-EDI (although the results are comparable). This can be explained by the higher combustion rates, and at some points, marginally more advanced spark timings (Figure 4a), which helps to advance the combustion phasing.

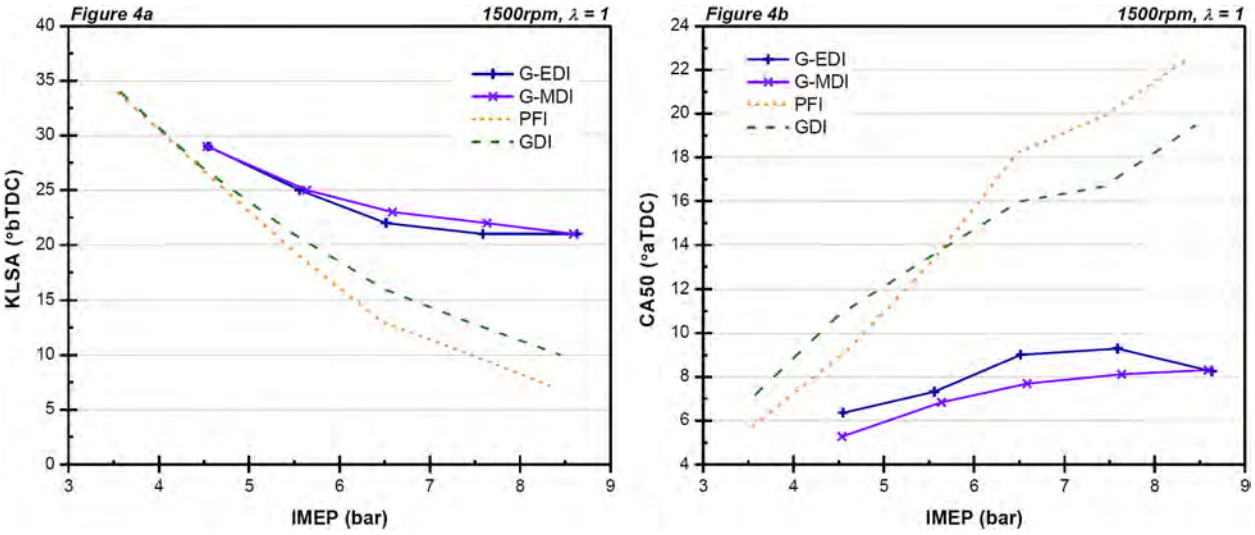

Figure 4. MBT spark timings (a) and CA50 (b) for G-EDI and G-MDI compared to PFI and GDI

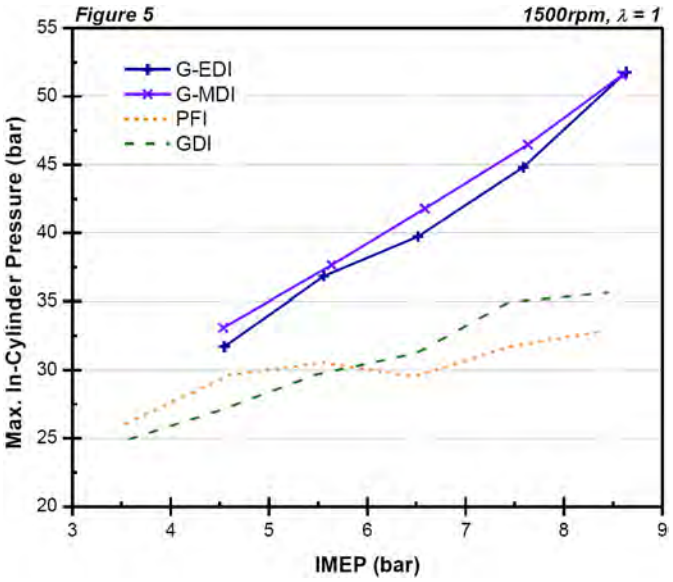

Figure 5. Maximum in-cylinder pressures for G-EDI and G-MDI compared to PFI and GDI

The combustion duration for G-EDI and G-MDI is compared to PFI and GDI in Figure 6 and is defined as the CAD from 10-90% MFB. Clearly, the addition of these lower alcohols dramatically reduces the combustion duration, which helps to explain the increase in P_{max}. At 4.5 bar IMEP, only 20% of ethanol is required in G-EDI in order to match the combustion duration of PFI. As the load increases, the combustion duration reduces further when compared to PFI and GDI. At 7.5 bar IMEP, despite injecting less than 45% of the total fuel volume (see Figure 3a), the lower alcohols reduce the combustion duration by 3 CAD over the lowest for gasoline (in DI). At 8.5 bar IMEP, the combustion duration when using G-EDI and G-MDI decreases by another 1 CAD. This further increases the separation with GDI to almost 5 CAD. With G-MDI, the combustion duration is consistently lower than with G-EDI (up to 1.8 CAD). This is because of the higher burning rate of methanol due to the higher oxygen content, as found by other researchers [32, 33, 34]. The combustion phase of G-MDI is also more advanced than G-EDI, as shown by the CA50 location in Figure 4b. Therefore, the fuel is burned during a period of lower change of in-cylinder volume, which results in a higher increase in pressure [29, 30], as seen in Figure 5.

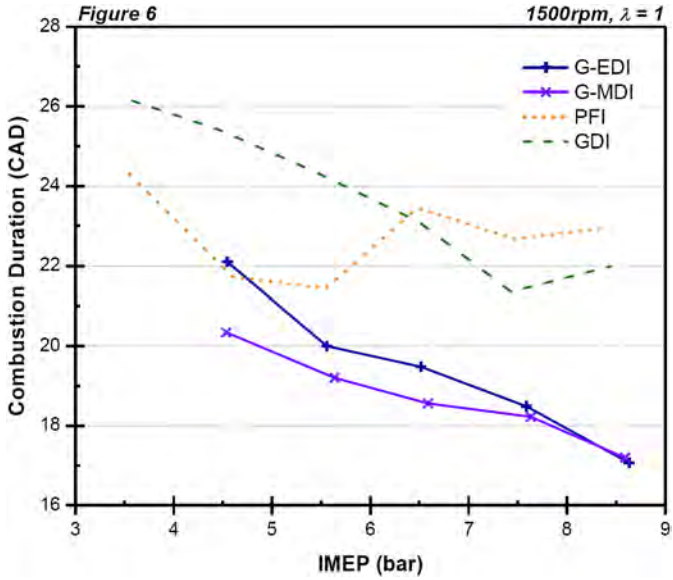

Figure 6. Combustion durations for G-EDI and G-MDI compared to PFI and GDI

Indicated and Fuel Efficiency

The indicated efficiency and volumetric indicated specific fuel consumption (ISFC) provide a good method of comparison between the overall benefits of G-EDI and G-

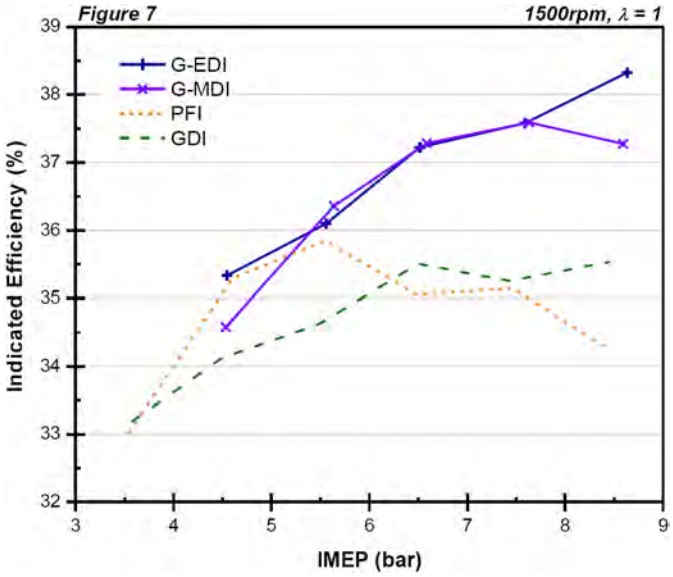

Figure 7. Indicated efficiency for G-EDI and G-MDI compared to PFI and GDI

MDI. The results for these tests are shown in Figure 7. Although the results for G-EDI and G-MDI are comparable, there are subtle differences. For instance, up to 5.5 bar IMEP, there is marginal change in indicated efficiency when using both lower alcohols in dual-injection from PFI, as shown in Figure 7. However, when above this load the indicated efficiency of the dual-injection cases increases similarly up to 7.5 bar IMEP. At this point, the indicated efficiency of G-EDI begins to exceed that with G-MDI and reaches a maximum of 38.3% at 8.5 bar IMEP, which is 1% higher than the maximum achieved with G-MDI (found at 7.5 bar IMEP). The decrease for G-MDI at 8.5 bar IMEP might be due to the lower volume fraction of methanol in DI compared to ethanol in DI at this load (Figure 3a) as the indicated efficiency of the gasoline (in PFI) that replaces the methanol would be lower. At this point, only 43% of methanol in DI is required to reach the MBT timing for MDI, whereas with G-EDI, this increases to 51% (Figure 3a). This is possibly due to the greater charge-cooling effect of methanol, requiring less fuel in order to suppress the knock.

The volumetric ISFC is shown in Figure 8a. As the ethanol and methanol DI volume fractions (Figure 3a) and indicated efficiencies (Figure 7) are quite similar, the difference in ISFC is due to the difference in LCV. For methanol, whose LCV is 26% lower than ethanol (Table 2), the ISFC increases above that with G-EDI by an average of 9.3% across the entire load range. At 8.5 bar IMEP, the ISFC for G-EDI is 9.7% higher than that with GDI (the lowest for gasoline), whereas with G-MDI this increase is over double, at 20.2%. Clearly, the use of ethanol as a dual-injection fuel would require less refueling in a real-world situation than with methanol. However, the effectiveness of both lower alcohols is shown in Figure 8b using the gasoline equivalent ISFC, herein termed ISFCE, as described in previous work by the authors [35]. Although the trend with ISFCE is inversely proportional to the trend with indicated efficiency in Figure 7, this gravimetric gasoline equivalent ISFC allows the fuel consumption efficiency of the different combustion modes to be compared on level terms. Above 5.5 bar IMEP, dual-injection produces lower ISFCE. At 7.5 bar IMEP, where the ISFCE for G-EDI and G-MDI are equal, the ISFCE is 223 g/kWh, 6.3% lower than GDI. This reduced energy demand (as shown in Figure 3b) also contributes to lower engine-out CO_2 emissions, as discussed in the next section.

Gaseous Emissions

The engine-out emissions of PFI and GDI are compared to G-EDI and G-MDI at the various loads and spark timings. Firstly, the traditional legislated emissions are evaluated, including the HC, NO_x and CO emissions, followed by an analysis of the carbon dioxide (CO_2) emissions.

As shown in Figure 9a, the isHC emissions for the lower alcohol cases are much lower than that with gasoline (PFI and GDI). The impact on the isHC emissions when using G-MDI is, on average, 22% lower than with G-EDI, and 48% lower than gasoline in PFI. This difference between the lower alcohols is likely due to the higher oxygen content of methanol (see Table 2) which aids the oxidation of unburned hydrocarbons as oxygen is more readily available. However, the reduced sensitivity of the FID analyzer to oxygenated fuels suggests that the isHC emissions for ethanol and methanol are higher than the values from the FID measurement [36, 37]. Therefore, if the HC emissions were assumed to be unburned fuel, FID response factors could be used to better approximate the isHC emissions of G-EDI and G-MDI. For ethanol and methanol, typical FID response factors are 0.7 and 0.4 [38, 39]. These factors have been applied to the dual-injection data in Figure 9a and are shown as corrected isHC emissions in Figure 9b.

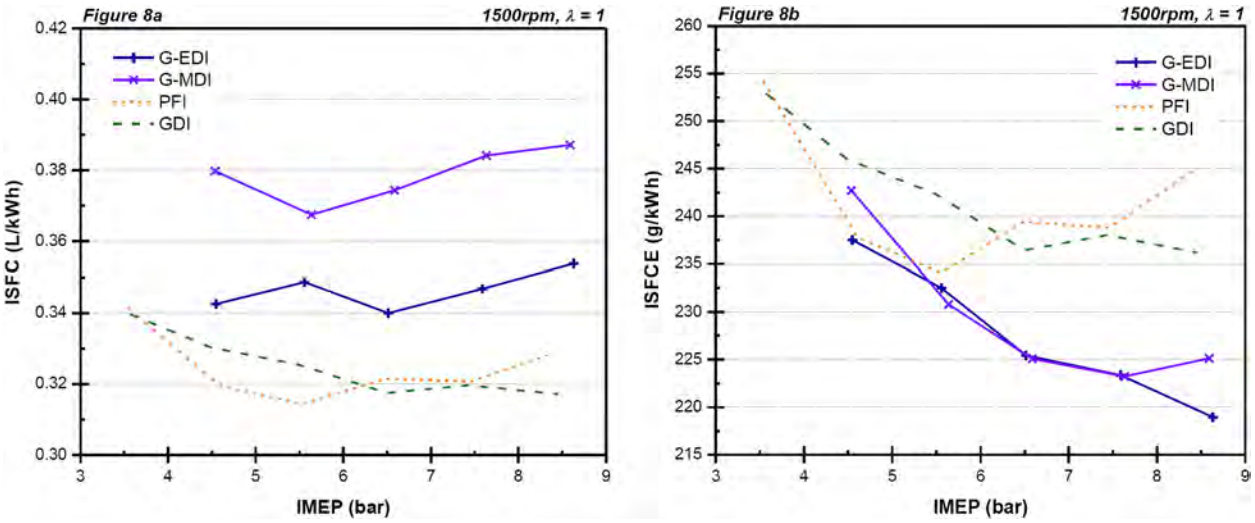

Figure 8. Indicated specific (volumetric) (a) and (gravimetric) gasoline equivalent (b) fuel consumption for G-EDI and G-MDI compared to PFI and GDI

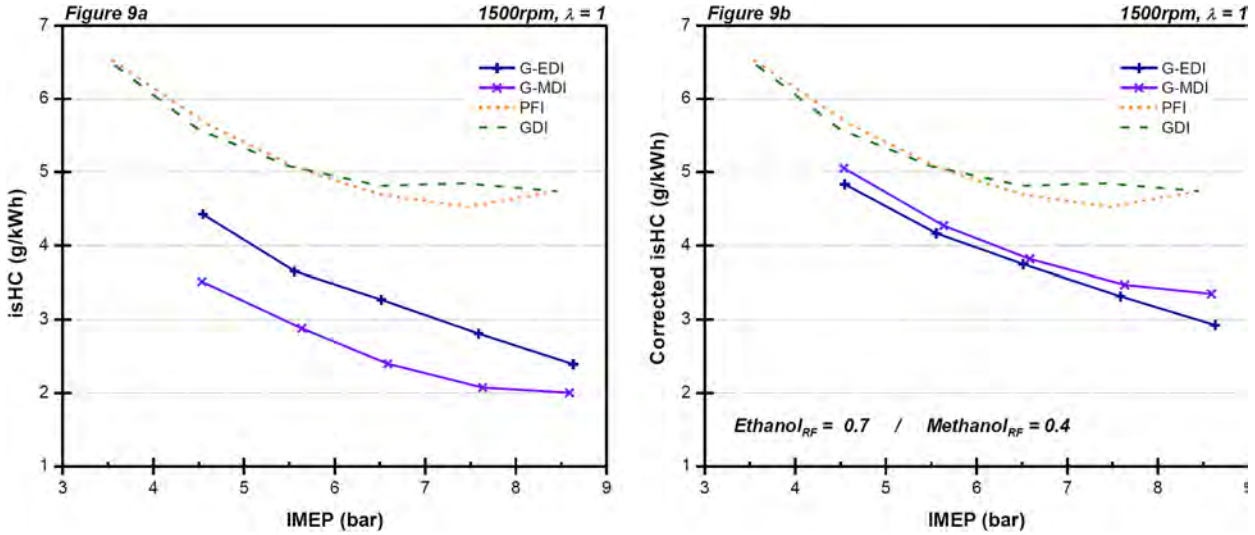

Figure 9. Uncorrected (a) and corrected (b) indicated specific hydrocarbon emissions for G-EDI and G-MDI compared to PFI and GDI

On a corrected HC basis, the isHC emissions from G-EDI and G-MDI are more comparable and still offer a reduction from the PFI and GDI case. However, this simplified correction does not correspond to a true HC quantification. This is because the HC emissions include various HCs, each with different FID sensitivity (also specific to the instrument). For instance, the dominant oxygenated product of combustion of ethanol and methanol after unburned fuel, is acetaldehyde and formaldehyde, respectively [40]. Both of these oxygenated HCs produce a lower FID response factor than the fuel itself [38] and so would further increase the corrected isHC emissions. Therefore, in order to accurately quantify the isHC emissions, a detailed HC speciation investigation must be carried out. This is, however, outside the scope of the current work.

The emissions of $isNO_x$ are shown in Figure 10. It is well publicized that the formation of NO_x increases very strongly with combustion temperature, which itself is related to the combustion pressure [29, 30]. Therefore, the production of $isNO_x$ increases with load. The separation between G-EDI and G-MDI is due to the higher combustion pressures with G-MDI (Figure 5), which is likely to cause higher combustion temperatures. As an example, at 8.5 bar IMEP the $isNO_x$ emissions when using the lower alcohols in dual-injection is 14% and 28% higher than with PFI and GDI, respectively. This clearly is the consequence of dual-injection. The higher

combustion temperatures caused by the gasoline component in PFI (little charge-cooling) and the more advanced spark timing when using the lower alcohols, both contribute to increasing the isNO_x production. However, when operating at stoichiometry with a three-way catalyst (TWC), the NO_x emissions will be dramatically reduced as the conversion efficiency is extremely high.

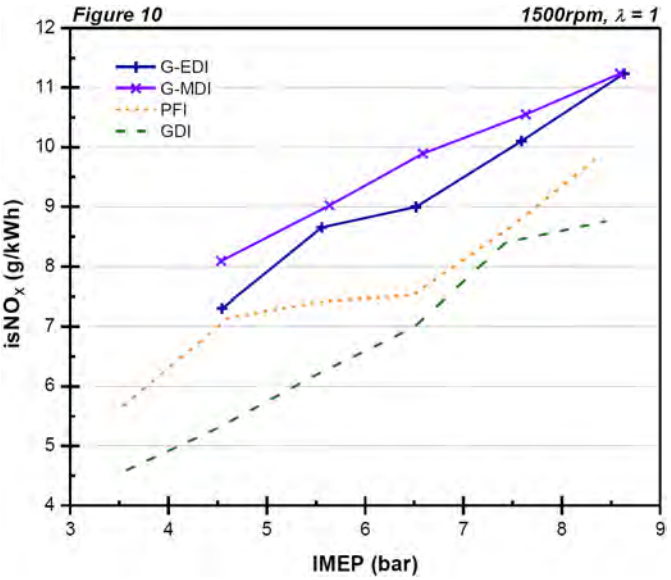

Figure 10. Indicated specific NO_x emissions for G-EDI and G-MDI compared to PFI and GDI

The indicated specific carbon monoxide emissions (isCO) comparison is made in Figure 11. Here, the dual-injection isCO emissions are always lower than GDI. Compared to PFI, the isCO emissions fluctuate within a similar range up to 6.5 bar IMEP, however, when the load increases, the dual-injection isCO emissions remain low (for both lower alcohols). The improved oxidation is due to more advanced spark timing, which helps to increase the combustion efficiency. The oxygen within the lower alcohol fuels also promotes oxidation as the oxygen molecules are more readily available. Also, the pre-mixed (homogeneous) PFI component is likely to be fully vaporized prior to ignition. Therefore, any localized fuel droplets injected in DI will benefit from the burning of gasoline PFI fuel vapor and further contribute to reduced isCO emissions. Although primary use of PFI produces high isCO emissions at higher loads (due to spark retard), its use as a supplement to the DI fuel helps to reduce the isCO emissions.

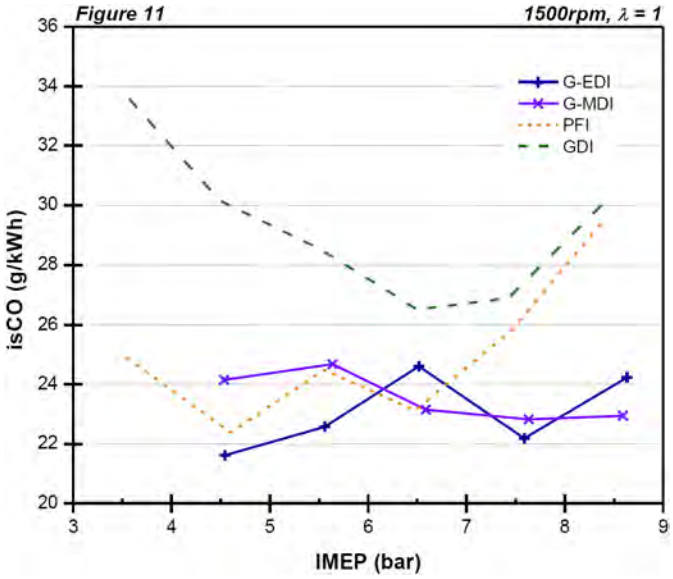

Figure 11. Indicated specific CO emissions for G-EDI and G-MDI compared to PFI and GDI

Finally, a consideration of the indicated specific CO_2 (isCO_2) production is made in Figure 12. Although CO_2 is a non-toxic gas, which is not classified as a pollutant engine emission, it is one of the substances responsible for global temperature rises through the greenhouse effect. The reduction of its emissions at higher engine loads was also one of the drivers for automobile OEMs switching from PFI to GDI operation in recent years [41]. The isCO_2 emissions are reduced with dual-injection over GDI for almost every load, as shown in Figure 12. The critical load is 5.5 bar IMEP. Above this, GDI emits lower isCO_2 emissions than PFI but the dual-injection results with the lower alcohols reduce this even further. At 8.5 bar IMEP, the isCO_2 emission with G-EDI is 775 g/kWh, which is 42 g/kWh (5%) less than with GDI. This result shows the effectiveness of dual-injection to combat CO_2 emissions: the higher the lower alcohol content, the greater the CO_2 reduction, as shown by the reduced carbon intensity in Table 2. Furthermore, there is the potential added benefit of consuming CO_2 during the raw production of ethanol and methanol when taken from biomass. Therefore, if the lifecycle CO_2 emissions were compared, the dual-injection strategy would look favorable.

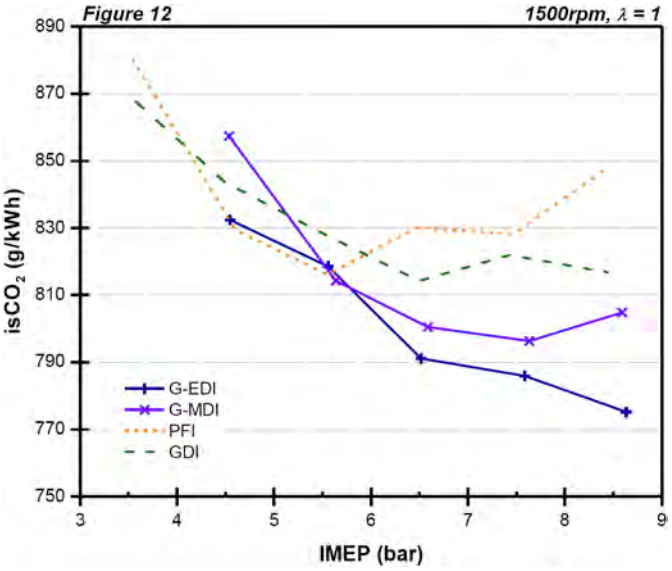

Figure 12. Indicated specific CO_2 emissions for G-EDI and G-MDI compared to PFI and GDI

CONCLUSIONS

In summary, this study investigates the benefit of dual-injection as a knock mitigation strategy for gasoline in PFI using minimum injections of ethanol or methanol in DI. The engine performance and emissions are compared under homogenous operation at various engine loads from 3.5 bar to 8.5 bar IMEP in 1 bar intervals. All tests were performed on a single cylinder DISI engine capable of running PFI and DI simultaneously and generating instantaneous changes in blend ratios. Based on these experiments, the following conclusions can be drawn:

i. The high latent heat of vaporization of ethanol and methanol dramatically mitigates the knock found with PFI. For instance, at 7.5 bar IMEP, the minimum DI volume fractions with G-EDI and G-MDI are only 41% and 43%, respectively permit a spark advance of 11-12 CAD relative to PFI. On an energy input basis, these DI volume fractions equate to 32% and 27% of the overall blend LCV, which is a consequence of the higher octane number and heat of vaporization of methanol. At 8.5 bar IMEP, this energy fraction increases to 41% with G-EDI, whereas it remains at 27% with G-MDI.

ii. The increased spark timing with low dual-injection blends lowers the combustion duration by up to 5 CAD over GDI. Due to the higher oxygen content of methanol, the combustion duration with G-MDI is up to 1.8 CAD lower than G-EDI.

iii. Above 5.5 bar IMEP, the indicated efficiency is higher with G-EDI and G-MDI than with PFI or GDI. Up to 7.5 bar IMEP the indicated efficiency of G-EDI and G-MDI are similar (37.6%, 2.3% higher than GDI). At 8.5 bar IMEP, however, the indicated efficiency of G-EDI is 38.3%, 1% higher than G-MDI and 2.8% higher than GDI, due to the higher content of ethanol, and therefore oxygen content, required to reach borderline knock.

iv. Reductions in HC, CO and CO_2 emissions are found at almost every load when using G-EDI and G-MDI compared to PFI and GDI. At 8.5 bar IMEP, the isCO_2 emissions are 5% lower with G-EDI than with GDI. However, these reductions vary between the lower alcohols. At the lowest load (4.5 bar IMEP) G-MDI produces 21% lower isHC emissions than G-EDI. In terms of isCO_2 emissions, G-EDI produces 2.9% lower emissions than G-MDI.

v. The consequence of more advanced spark timing with G-EDI and G-MDI is higher combustion pressures (and temperatures), which increases the NO_x emissions. At 8.5 bar IMEP, the isNO_x emissions increase by up to 14% over PFI.

Overall, these experiments highlight the effectiveness of ethanol and methanol as dual-injection fuels. On an energy basis, methanol is more effective than ethanol; lower methanol fractions are required for the same engine load as a consequence of the higher charge-cooling effect. However, the higher energy density of ethanol offers higher fuel economy effectiveness (reduced fuel consumption) and reduced CO_2 emissions. These results are contrary to the simulations by EBS, who predicted that almost half the amount of methanol is required compared to E85 in order to reach borderline knock despite the 30% deficiency in energy density [26]. This was largely due to the improved anti-knock and charge-cooling properties of methanol.

Therefore, future engine investigations are planned to supplement these findings and examine the case for methanol and other oxygenated fuels. This includes an assessment of the effectiveness of fixed fuel blends in dual-injection compared to DI, various modeling and optical engine studies, as well as a full investigation into the unregulated and toxic emissions. Furthermore, the authors plan to investigate the effect on particulate matter (PM) emissions in order to better understand the benefits in PM emissions reduction as recently announced by Audi [24].

REFERENCES

1. Allen, M., Frame, D., Frieler, K., Hare, W., Huntingford, C., Jones, C., Knutti, R., Lowe, J., Meinshausen, M., Meinshausen, N. and Raper, S., *The Exit Strategy*, Nature Reports. 2009. p.56-58.
2. Shell, *Shell Energy Scenarios to 2050*, Signals and Signposts. 2011, Shell International BV: The Hague.
3. Brevitt, B., *Alternative Vehicle Fuels*, Science and Environment. 2002, House of Commons Library: London.
4. White, T., "Alcohol as a Fuel for the Automobile Motor," SAE Technical Paper 070002, 1907, doi: 10.4271/070002.
5. DIRECTIVE 2009/28/EC. *On the Promotion of the use of Energy from Renewable Sources*. Official Journal of the European Union, 2009.
6. Curtis, B., *U.S. Ethanol Industry: the Next Inflection Point*. Energies and Resource Group, Year in Review, 2008.
7. Goldemberg, J., *The Challenge of Biofuels*. Energy & Environmental Science, 2008. 1(5): p.523-525.
8. Demirbas, A., *Progress and Recent Trends in Biofuels*. Progress in Energy and Combustion Science, 2007. 33(1): p.1-18.
9. Demirbas, A., *Competitive liquid biofuels from biomass*. Applied Energy, 2011. 88(1): p.17-28.

10. OECD, Organisation for Economic Co-operation and Development, *Biofuel Support Policies: An Economic Assessment*. 2008: Paris.
11. Agarwal, A.K., *Biofuels (Alcohols and Biodiesel) Applications as Fuels for Internal Combustion Engines*. Progress in Energy and Combustion Science, 2007. 33(3): p.233-271.
12. Demirbas, M.F., *Biorefineries for Biofuel Upgrading: A Critical Review*. Applied Energy, 2009. 86(1): p.151-161.
13. Dolan, G., *China Takes Gold in Methanol Fuel*. Journal of Energy Security, 2008.
14. Kowalewicz, A., *Methanol as a Fuel for Spark Ignition Engines: a Review and Analysis*. Proceedings of the IMechE, 1993. 207(1): p. 43-52.
15. Liu, S., Clemente, E.R.C., Hu, T. and Wei, Y., *Study of Spark Ignition Engine Fueled with Methanol/Gasoline Fuel Blends*. Applied Thermal Engineering, 2007. 27: p.1904-1910.
16. Wei, Y., Liu, S., Li, H., Yang, R., Liu, J. and Wang, Y., *Effects of Methanol/Gasoline Blends on a Spark Ignition Engine Performance and Emissions*. Energy and Fuels, 2008. 22: p.1254-1259.
17. Nakajima, S., Saiki, R., and Goryozono, Y., "Development of an Engine for Flexible Fuel Vehicles (FFV)," SAE Technical Paper 2007-01-3616, 2007, doi:10.4271/2007-01-3616.
18. Bromberg, L., Cohn, D.R., and Heywood, J.B., *Water Based Systems for Direct Injection Knock Prevention in Spark Ignition Engines*. U.S. Patent, 2010: US 2010121559, United States Patent and Trademark Office.
19. Cohn, D.R., Bromberg, L., and Heywood, J.B., *Fuel Management System for Variable Ethanol Octane Enhancement of Gasoline Engines*, U.S. Patent, 2010: US 2010175659, United States Patent and Trademark Office.
20. Cohn, D.R., Bromberg, L., and Heywood, J.B., *Direct Injection Ethanol Boosted Gasoline Engines: Biofuel Leveraging For Cost Effective Reduction of Oil Dependence and CO2 Emissions*. 2005, Massachusetts Institute of Technology: Cambridge, MA.
21. Stein, R., House, C., and Leone, T., "Optimal Use of E85 in a Turbocharged Direct Injection Engine," *SAE Int. J. Fuels Lubr.* 2(1): 670-682, 2009, doi:10.4271/2009-01-1490.
22. Whitaker, P., Shen, Y., Spanner, C., Fuchs, H. et al., "Development of the Combustion System for a Flexible Fuel Turbocharged Direct Injection Engine," *SAE Int. J. Engines* 3(1):326-354, 2010, doi: 10.4271/2010-01-0585.
23. Ikoma, T., Abe, S., Sonoda, Y., Suzuki, H. et al., "Development of V-6 3.5-liter Engine Adopting New Direct Injection System," SAE Technical Paper 2006-01-1259, 2006, doi:10.4271/2006-01-1259.
24. Wurms, R., Jung, M., Adam, S., Dengler, S., Heiduk, T. and Eiser, A., *Innovative Technologies in Current and Future TFSI Engines from Audi*, 20th Aachen Colloquium Automobile and Engine Technology 2011. 2011.
25. Bromberg, L. and Cohn, D., "Alcohol Fueled Heavy Duty Vehicles Using Clean, High Efficiency Engines," SAE Technical Paper 2010-01-2199, 2010, doi:10.4271/2010-01-2199.
26. Blumberg, P., Bromberg, L., Kang, H., and Tai, C., "Simulation of High Efficiency Heavy Duty SI Engines Using Direct Injection of Alcohol for Knock Avoidance," *SAE Int. J. Engines* 1(1):1186-1195, 2009, doi: 10.4271/2008-01-2447.
27. Sandford, M., Page, G., and Crawford, P., "The All New AJV8," SAE Technical Paper 2009-01-1060, 2009, doi:10.4271/2009-01-1060.
28. Wu, X., Daniel, R., Tian, G., Xu, H., Huang, Z. and Richardson, D., *Dual-Injection: the Flexible Bi-Fuel Concept for Spark-Ignition Engines Fuelled with Various Gasoline and Biofuel Blends*. Applied Energy, 2011. 88: p.2305-2314.
29. Heywood, J.B., *Internal Combustion Engine Fundamentals*. 1988: McGraw-Hill.
30. Stone, R., *Introduction to Internal Combustion Engines*. Third Edition. 1999: Macmillan Press.
31. Zhu, G.G., Haskara, I. and Winkelman, J., *Closed-Loop Ignition Timing Control for SI Engines Using Ionization Current Feedback*. IEEE Transactions on Control Systems Technology, 2007. 15(3): p.12.
32. Gülder, O.L., *Laminar Burning Velocities of Methanol, Ethanol and Isooctane-Air Mixtures*. The Combustion Institute, 1982. Laminar Flames II: p.275-281.
33. Beeckmann, J., Röhl, O., and Peters, N., "Experimental and Numerical Investigation of Iso-Octane, Methanol and Ethanol Regarding Laminar Burning Velocity at Elevated Pressure and Temperature," SAE Technical Paper 2009-01-1774, 2009, doi:10.4271/2009-01-1774.
34. Vancoillie, J., Verhelst, S., and Demuynck, J., "Laminar Burning Velocity Correlations for Methanol-Air and Ethanol-Air Mixtures Valid at SI Engine Conditions," SAE Technical Paper 2011-01-0846, 2011, doi:10.4271/2011-01-0846.
35. Daniel, R., Tian, G., Xu, H., Wyszynski, M. L., Wu, Z. and Huang, Z., *Effect of Spark Timing and Load on a DISI Engine Fuelled with 2,5-Dimethylfuran*. Fuel, 2011. 90: p. 449-458.
36. Cheng, W.K., Summer, T. and Collings, N., *The Fast-response Flame Ionization Detector*. Progress in Energy and Combustion Science, 1998. 24: p.89-124.
37. Wallner, T. and Miers, S., "Combustion Behavior of Gasoline and Gasoline/Ethanol Blends in a Modern Direct-Injection 4-Cylinder Engine," SAE Technical Paper 2008-01-0077, 2008, doi: 10.4271/2008-01-0077.
38. Wallner, T., *Correlation Between Speciated Hydrocarbon Emissions and Flame Ionization Detector Response for Gasoline/Alcohol Blends*. Journal of Engineering for Gas Turbines and Power, 2011. 133(8).
39. Grob, R.L., *Modern Practice of Gas Chromatography*. Second Edition: 1985: John Wiley and Sons, Inc.
40. Magnusson, R. and Nilsson, C., *The Influence of Oxygenated Fuels on Emissions of Aldehydes and Ketones from a Two-Stroke Spark Ignition Engine*. Fuel, 2011. 90: p. 1145-1154.
41. Zhao, F., Harrington, D.L., and Lai, M.-C. D., "Automotive Gasoline Direct-Injection Engines," Society of Automotive Engineers, Inc., Warrendale, PA, ISBN 978-0-7680-0882-1, 2002.

CONTACT INFORMATION

Professor Hongming Xu
School of Mechanical Engineering
University of Birmingham, Edgbaston
United Kingdom, B15 2TT
Tel: +44 (0)121 414 4153
h.m.xu@bham.ac.uk

ACKNOWLEDGMENTS

The present work is part of a 3-year research project sponsored by the Engineering and Physical Sciences Research Council (EPSRC) under the grant EP/F061692/1. The authors would like to acknowledge the support from Jaguar Cars Ltd, Shell Global Solutions and various research assistants and technicians especially Xuesong Wu and Shahrouz Norouzi. The authors are also grateful for the financial support from the European Regional Development Fund (EUDF) and Advantage West Midlands (AWM). Finally, the authors would like to acknowledge the support from their international collaborators at Tsinghua University, China.

DEFINITIONS

aTDC
After Top Dead Centre
bTDC
Before Top Dead Centre
CA50
Crank Angle Degrees of 50% MFB
CAD
Crank Angle Degrees
CO
Carbon Monoxide
CO_2
Carbon Dioxide
COV
Coefficient of Variation
DI
Direct-Injection
DISI
Direct-Injection Spark Ignition
E85
15% Gasoline and 85% Ethanol by Volume
EBS
Ethanol Boosting Systems

ETH
Ethanol
GDI
Gasoline Direct-Injection
G-EDI
Ethanol Dual-Injection (Gasoline in PFI and Ethanol in DI)
G-MDI
Methanol Dual-Injection (Gasoline in PFI and Methanol in DI)
HC
Hydrocarbon
IMEP
Indicated Mean Effective
isCO
Indicated Specific Carbon Monoxide
isCO_2
Indicated Specific Carbon Dioxide
ISFC
Indicated Specific Fuel Consumption (volumetric)
ISFCE
Indicated Specific Fuel Consumption (gasoline) Equivalent (gravimetric)
isHC
Indicated Specific Hydrocarbons
isNO_x
Indicated Specific Nitrogen Oxides
KLSA
Knock Limited Spark Advance
LCV
Lower Calorific Value
MBT
Maximum Brake Torque
MFB
Mass Fraction Burned
MTH
Methanol
NO_x
Nitrogen Oxides
PFI
Port Fuel Injection
PM
Particulate Matter
RPM
Revolutions per Minute
SGDI
Spray-Guided Direct-Injection
SI
Spark Ignition
SOI
Start of Injection
TDC
Top Dead Centre
TWC
Three-way Catalyst
ULG
Unleaded Gasoline